International Journal of Mechanical and Industrial Engineering

Volume 2 | Issue 4 Article 10

April 2013

ANALYSIS OF SPOT WELDING ELECTRODE

RAJANARENDER REDDY PINGILI
ME Advanced Design and Manufacturing. Vasavi College of Engineering, Hyderabad.,
rajanarender69@yahoo.com

ANALYSIS OF SPOT WELDING ELECTRODE

RAJANARENDER REDDY PINGILI

ME Advanced Design and Manufacturing. Vasavi College of Engineering, Hyderabad.
E.mail: rajanarender69@yahoo.com

Abstract: - Electric resistance spot welding has been extensively used for many years in the automotive and aerospace industry for joining body sheet components. Compared to other welding processes such as arc welding process, resistance spot welding is fast, easily automated and easily maintained. Accurate thermal analysis of spot welding electrode could permit critical design parameters to be identified for improved electrode life. It is a complex process where coupled interactions exist between electrical, thermal and mechanical phenomena. On the other hand, finite element method (FEM), which can deal with nonlinear behaviors and complex boundary conditions, provides a powerful tool for studying these interactions and has become the most important method for the analysis of resistance spot welding. In this study, a 2-D finite element model has been developed to predict the transient thermal behavior of spot welding electrodes. The model included heat transfer analysis, electrical field analysis and phase change during melting or solidification and temperature dependant material properties, and also their inter-dependence. The contacts at faying surface and at electrode – work interface, with temperature dependant contact resistances were modeled. Three types of electrode shapes – flat, pointed and dome nose were analyzed. Temperature distribution on each electrode shape was obtained from the finite element analysis. Maximum temperature of 2876 ºC was observed in dome nose electrode in 0.2 seconds of welding time. Dome nose electrode requires a minimum weld time of all the other electrode shapes to get the required nugget size, resulting in the least power consumption. Nugget size was predicted for each electrode shape. Experimental results obtained were in good agreement with the finite element analysis results.

1. WELDING CYCLE

All resistance welding operations are automatic and therefore all process variables are preset and maintained constant. Once a welding operation has been initiated, the weld cycle is completed as per the preset times. Welding cycle for spot welding consists of four elements viz., squeeze stage, weld stage, hold stage and off stage. These stage timings are fixed for a particular metal and a thickness range. Each of these phases plays a vital role in achieving a sound weld of the required size.

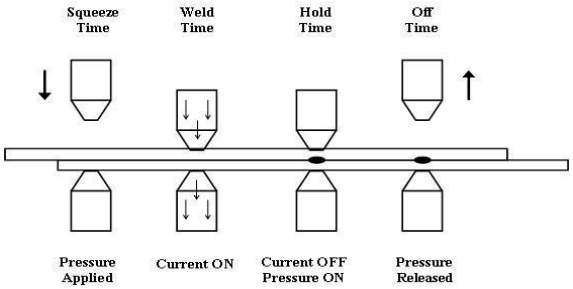

Fig. Welding cycle

2. WELDING PARAMETERS

The welding current, time of current flow and the electrode force are recognized as the fundamental variables of resistance spot welding. For achieving quality welds in most metals, these variables are required to be kept within very close limits.

2.1 Welding current

The size of the weld nugget depends upon the rate of internal heat generation. Thus welding current is the most critical variable. Accurate control of welding current is imperative for the success of resistance welding.

The suitable current density can be determined by the following relationship.

$$J = 192 + k_c e^{-ts} \qquad (2)$$

Where J = Current density in A/mm^2

t_s = sheet thickness in mm

k_c = constant equal to 480 for mild steel

e = constant, 2.718

2.2 Weld time

Weld time is the time during which welding current is applied to the metal sheets. Weld time should be as short as possible. The time of current flow is controlled by electronic, mechanical, manual or pneumatic timers. The weld time might have to be adjusted to fit the welding equipment in case it does not fulfil the requirements for the weld current and the electrode force.

2.3 Electrode force

The purpose of the electrode force is to squeeze the metal sheets to be joined together. The electrode force serves a number of functions such as bringing the work pieces in close contact, reducing the initial contact resistance at the interfaces and consolidating the molten metal into a sound weld nugget. The electrode force is applied by hydraulic, pneumatic, magnetic, or mechanical means.

3. RESISTANCE WELDING EQUIPMENT

The main features of the resistance spot welding equipment are electrical circuit, contactors and timers, and a mechanical system as shown in Fig..

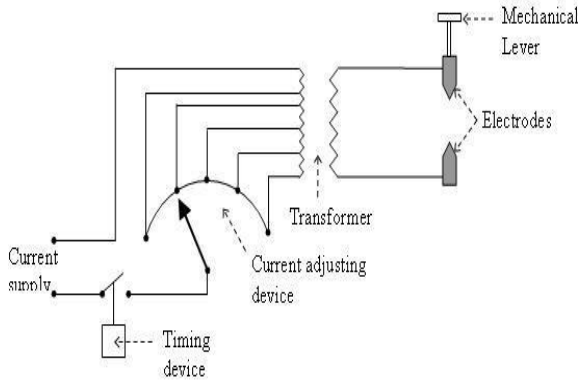

Fig. Resistance spot welding

4. ELECTRODE CHARACTERISTICS

4.1 Functions Of Electrode

1. To conduct the welding current to the work pieces.
2. To withstand and to transmit the necessary force to the work pieces to produce satisfactory weld.
3. To dissipate a part of the heat from the work and thus prevent surface fusion.

4.2 Composition Of Electrode Material

Despite high electrical and thermal conductivities, pure copper is soft and easily deforms under load, and therefore cannot be used as electrode material. Metals such as tellurium and nickel are added to impart strength to the material.

Table 1. Material composition of electrode

Element	% of composition
Copper	98.4%
Tellurium	0.5%
Nickel	1.1%

4.3 Electrode Shapes

To achieve the desired current density, it is important to have proper electrode shape. For this purpose, three main types of electrodes are commercially available.

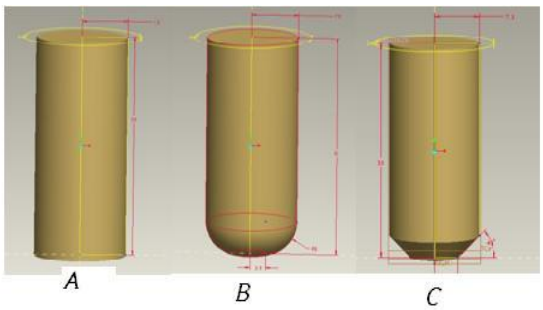

Fig. 6.1. Different electrode geometries: A – Flat, B – Dome nose, C - Point

4.4 Electrode Size

The electrode tip diameter depends upon the required nugget diameter. The nugget diameter is decided by the sheet thickness to be welded. The electrode tip size is considered nearly equal to the nugget size, which is found using Unwins formula

$$D_e = 6\sqrt{t} \qquad (1)$$

Where t is the sheet thickness in mm

D_e is electrode tip diameter

If the full length of the electrode is made of the same cross-section, it will be too weak to withstand the pressure to be exerted through it, and also causes high electric resistance resulting in overheating. Thus the pointed electrodes are made with truncated cone with an included angle of 120 to 140º, whereas sufficient radius is provided for domed electrode.

5. FINITE ELEMENT MODEL

The transient thermal analysis of the resistance spot welding process was modeled as a 2-D axisymmetric problem. Sheet metal of 1 mm thickness was modeled. Three models corresponding to different shapes of electrodes were modeled as follows:

1. Flat electrode of 15 mm diameter.
2. Pointed electrode of 15 mm diameter, and included angle of 120º.
3. Dome nose electrode with diameter of 15 mm, and a radius of curvature of 75 mm.

6. MATERIAL PROPERTY

The steel sheets in this study were mild carbon steel commonly used in automotive body assemblies. The material of the electrode is Copper-Tellurium alloy.

All the thermal properties of both the electrode and the work piece, such as thermal conductivity, specific heat, density, latent heat and enthalpy are given in Tables 1-3. [7] Phase change is taken into account by defining the enthalpy of the material as a function of temperature as given by the following equation.

$$H = \int \rho C(T)\, dT \qquad (1)$$

where ρ is the density of material in kg/m^3 and C(T) is the specific heat of the material in J/kg ºC as a function of temperature.

Table 1. Material properties (Thermal conductivity & Resistivity)

Temp. °C		21	93	204	316	427	538	649	760	871	982	1093	1204
Thermal Conductivity W/m-°C	Mild Steel	64.75	63.25	55.33	49.94	44.86	39.77	34.91	30.5	28.41	27.66	28.56	-
	Copper Electrode	390.3	380.6	370.1	355.1	345.4	334.9	320.0	315.5	310.3	305.0	300.1	-
Resistivity Ωm x 10^{-8}	Mild Steel	14.2	18.6	26.7	37.6	49.5	64.8	81.8	101.1	111.5	115.8	117.9	120.9
	Copper Electrode	2.64	3	4	5.05	6.19	6.99	8	8.98	9.48	9.98	-	-

Table 2. Material properties (Specific heat)

Temp. °C		21	93	204	316	427	538	649	732	760	774	799	1204
Specific Heat J/Kg- °C	Mild Steel	443.8	452.2	510.8	561.0	611.3	661.5	762.0	1004	2386	1004	1189	1189
	Copper Electrode	397.8	401.9	418.7	431.2	439.6	452.2	464.7	-	477.3	-	-	502.4

Table 3. Material properties (Enthalpy of Mild Steel)

Temp. °C	0	500	1000	1500	2000
Enthalpy J/m^3	0	2.5×10^9	5×10^9	1.3×10^{10}	1.75×10^{10}

Because the materials are subjected to a wide range of temperatures, these properties, except density and latent heat, are considered as temperature dependant. The electrical contact resistance has dominant effects on the formation of the weld nugget. It is important to appropriately treat the electrical contact resistance in the computational simulation. In this study, the contact resistance is described as a function of temperature. Density of mild steel is 7800 kg/m^3, and that of copper is 8900 kg/m^3.

7. MESHING

The coupled-field solid element PLANE 223 was employed to simulate the thermal-electrical interaction. This 2-D element is capable of accounting internal heat generation due to Joule heating. The element also accounts for both transient thermal and transient electrical effects. It has eight nodes with up to three degrees of freedom per node. Temperature and voltage were given as degrees of freedom for this analysis.

The contact pair elements CONTA 171 and TARGET 169 were employed to simulate the contact behaviors. TARGE169 is used to represent various 2-D "target" surfaces for the associated contact elements. The contact elements themselves overlay the solid elements describing the boundary of a deformable body and are potentially in contact with the target surface, defined by TARGE169. This target surface is discretized by a set of target segment elements and is paired with its associated contact surface via a shared real constant set. It has three nodes with up to five degrees of freedom per node. CONTA171 is used to represent contact and sliding between 2-D "target" surfaces and a deformable surface, defined by this element. Contact occurs when the element surface spenetrates one of the target segment elements on a specified target surface. It has two nodes with up to five degrees of freedom per node. There were three contact areas in the model. Contact areas 1 and 3 represented the electrode-work piece interface, and contact area 2 represented the faying surface as shown in Fig.

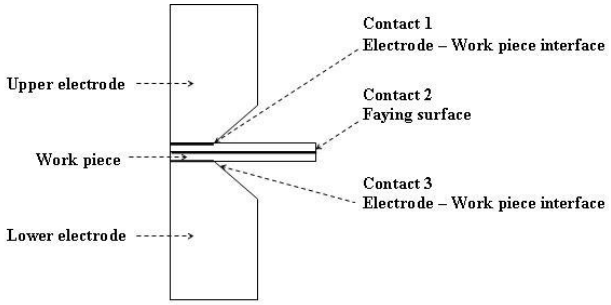

Fig. 7. Contact zones in the model

In order to obtain reliable results, fine meshes were generated near these contact areas, while other areas were relatively coarse, as shown in Fig.

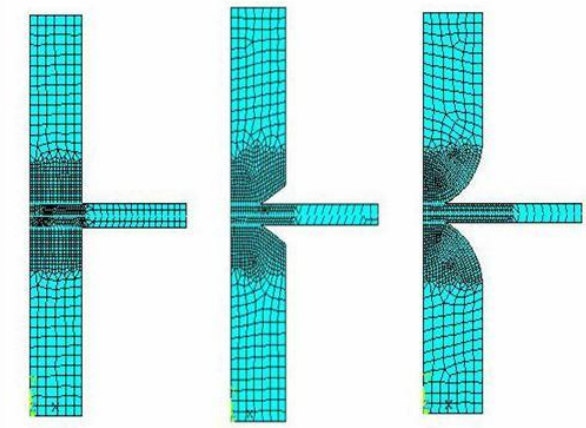

Fig. 8. Finite element models of different electrodes with mesh

8. LOADS APPLIED ON THE MODEL

8.1 Thermal load

Natural convection occurs at the surfaces exposed to the air. Thermal convection is given on the lateral surface of the electrodes and the portion of the work pieces exposed to air, with a convection co-efficient of 25 W/m^2 ºC, and a bulk temperature of 30 ºC. A uniform temperature of 30 ºC is provided as the initial condition on all the nodes of the model.

8.2 Electrical load

The input current in this simulation was AC 50 Hz sine wave of 12.5 kA applied for 0.2 seconds. In order to simulate the cooling process of the welding, the input current was set to zero after 0.2 seconds upto 0.6 seconds. The current was imposed as a nodal load on the top surface of the upper electrode. The pattern of the current is shown in Fig.

$$I = 6250 \times \sin(2\pi\omega t) \quad , \qquad 0 < t \leq 0.2$$

$$= 0 \qquad , \qquad t > 0.2$$

where I is the instantaneous current, ω is the frequency (50Hz) and t is time in seconds.

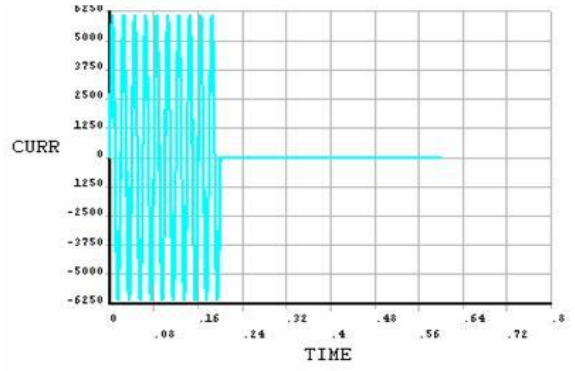

Fig. 9 Input Current as a function of time

9. CONTACT MODELING

In finite element code ANSYS contact wizard is used to manually establish the contact pairs. In this model three contact pairs were established- the faying surface which is the work piece–work piece interface and the electrode-work piece interface.

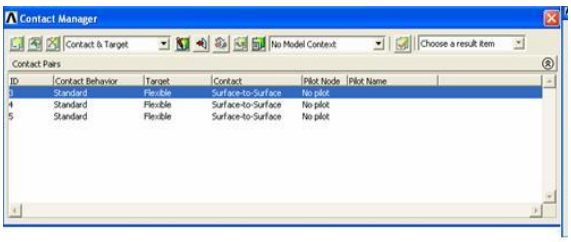

Fig. 10. Contact manager

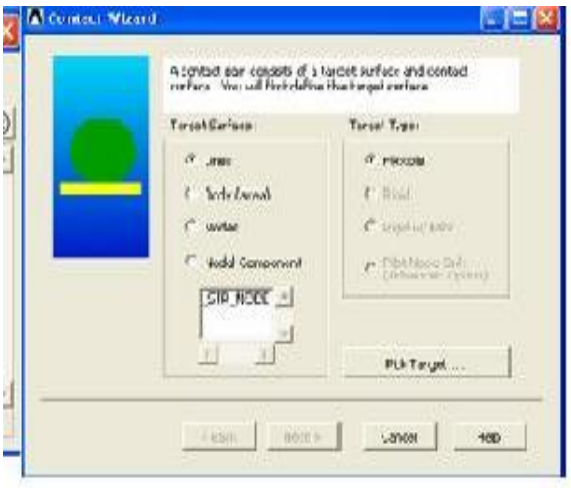

Fig. 11. Contact wizard

Using contact wizard the contact and target were specified using lines to form a single contact pair. The contact wizard allows selecting more than one area for target and contacting surface thus allowing multiple areas to form single contact surface. After the target and contact surfaces are specified, the properties of the contact pair namely electrical contact conductance and thermal contact conductance are given as input. The electrical contact conductance and thermal contact conductance are described as a function of temperature as shown in Fig. and Fig. respectively. The connectivity of the contact pairs are ensured by the command '*cncheck, adjust*', which physically move the contact nodes to the target surface.

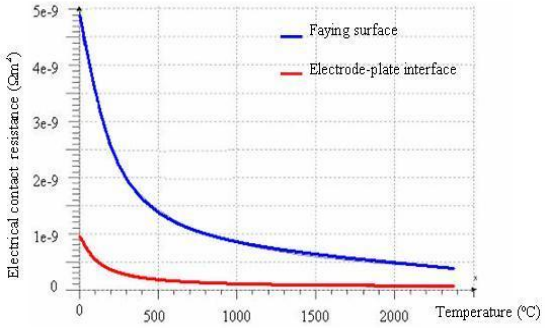

Fig. Electrical contact resistance

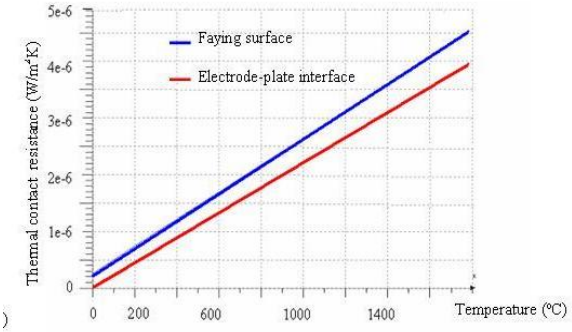

Fig. Thermal contact resistance

10. RESULTS AND DISCUSSION

The temperature fields for the three types of electrode shapes were obtained for an input current of 12.2 kA for 0.2 seconds welding time. The highest temperature was kept at the center of the faying surface throughout the whole welding process. Melting first occurred at the faying surface, and then expanded to the material near the faying surface.

10.1 Temperature Distribution

The results obtained from simulation and experiments are shown in Fig.

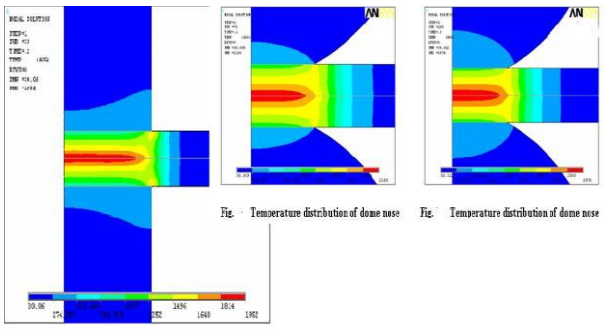

Fig. Temperature distribution of dome nose

Fig. Temperature distribution of dome nose

Fig. Temperature distribution of flat electrode at 0.2 s

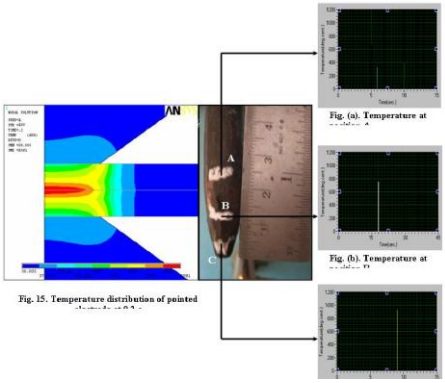

Fig. 15. Temperature distribution of pointed

In 0.2 seconds, the temperature in the flat electrode was found to be 510ºC at the electrode tip, and 1952ºC at the faying surface. In 0.2 seconds, temperature in the pointed electrode was observed as 706ºC at the tip, and 2091ºC at the faying surface. In 0.1 seconds, the temperature in the dome nose electrode was found to be 803ºC at the tip, and 2150ºC at the faying surface. In 0.2 seconds, the temperature in the dome nose electrode at the tip was 949ºC, and the faying surface was 2876ºC.

It was observed that for the same input current and weld time, the temperature obtained in the dome nose electrode is 2876 ºC, which was far higher than the other two shapes. The reduced contact area between the electrode and the work piece results in an increase in the current density. Moreover, the faying surface was found to have reached the required temperature within a meager time interval of 0.1 seconds. This trend in the temperature indicates that there is a scope for power saving, by terminating the input current after 0.1 seconds, unlike the other shapes. For same input current and weld time, the flat electrode was found to have produced the least temperature of all the electrode shapes.

10.2 Temperature History

The temperature history at the electrode tip obtained through the simulation for the three shapes of electrodes are shown in Fig..

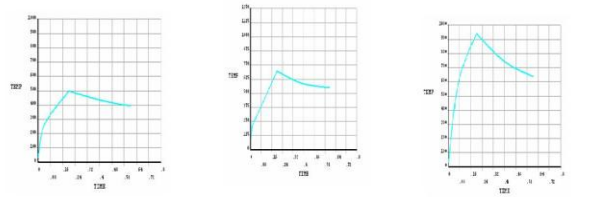

Fig. Temperature history of flat electrode for weld cycle Fig. Temperature history of pointed electrode for weld cycle Fig. Temperature history of dome nose electrode for we

11. CONCLUSIONS

From the work carried out on study of temperature fields in the electrodes used in electric resistance spot welding as discussed, the following conclusions are arrived at.

1. A thermal-electric 2-D finite element model has been developed to analyze the transient thermal behavior of resistance welding process.
2. The developed model considers the electric and thermal conduction in the solid, convection due to ambient air, latent heat of fusion due to solid-liquid phase change, and material properties as a function of temperature.
3. The thermal-electric contacts have been modeled with contact resistance as a function of temperature.
4. The thermal behavior of the three electrode geometries have been predicted from the thermal electric analysis.
5. The dome nose electrode is found to be better than the other shapes for resistance spot welding since it consumes the least power.
6. The maximum nugget diameter was produced by the flat electrode and the maximum depth of fusion was produced by the dome nose electrode.
7. The simulation results are in good agreement with the experimental results.
8. The methodology adopted in this work can be used while selecting parameters for a new product or part geometry that is to be welded using electric resistance spot welding.

REFERENCES

[1]. Huh.H., and Kang.W.J., 1997, "Electrothermal Analysis of Electric Resistance Spot Welding Process by a 3-D Finite Element Method", Journal of Materials Processing Technology, Vol.63, pp.672-677.

[2]. Feng.Z., et al, 1998, "An Incrementally Coupled Electrical-Thermal-Mechanical Model for Resistance Spot Welding", 5th International Conference on Trends in Welding Research, pp.1-6.

[3]. Yeung.K.S., and Thornton,P.H., 1999, "Transient Thermal Analysis of Spot Welding Electrodes", AWS Welding Journal, Vol.78, No.1, pp.1-6.

[4]. De.A., and Dorn.L., 2003, "Computer Simulation of Resistance Spot Welding Process",7th International Seminar on Numerical Analysis of Weldability, Austria.

[5]. Feulvarch.E., et al, 2006, "Resistance Spot Welding Process: Experimental and Numerical Modeling of the Weld Growth Mechanisms with Consideration of Contact Conditions", Journal of Numerical Heat Transfer, Part A, Vol.49: 1–23.

[6]. Neville Williams.T., "Resistance Spot Welding", ASM Handbook of Welding.

[7]. Zhigang.H., Yuanxung Wang, Chunzhi Li and Chuanyao Chen, 2006, "An Analysis of Resistance Spot Welding", AWS Welding Journal, pp.36-40.

[8]. Zhigang.H., et al, 2006, "A Study on Numerical Analysis of the Resistance Spot Welding Process", Journal of Achievements in Materials and Manufacturing Engineering, pp.140-145.

[9]. Zhigang.H., et al, 2007, "Finite Element Analysis for the Mechanical Features of Resistance Spot Welding Process", Journal of Materials Processing Technology, Vol.185, pp.160–165.

[10]. De.A., Thaddeus.M.P., and Dorn.L., 2003, "Numerical Modelling of Resistance Spot Welding of Aluminium Alloy", ISIJ International, Vol.43, No.2, pp.238–244.

[11]. De.A., 2002, "Finite Element Modelling of Resistance Spot Welding of Aluminium with Spherical Tip Electrodes", Journal of Science and Technology of Welding and Joining, Vol.7, No.2, pp.119-124.

[12]. Feulvarch.E., Robin.V., and Bergheau.J.M., 2004, "Resistance Spot Welding Simulation: A General Finite Element Formulation of Electrothermal Contact Conditions", Journal of Materials Processing Technology, pp.436–441.

[13]. Jamil Khan.A., Kirk Broach, and Arafin Kabir.A.A.S., 2000, "Numerical Thermal Model of Resistance Spot Welding in Aluminium", Journal of Thermophysics and Heat Transfer, Vol.14, No.1, January-March 2000.

[14]. Jamil Khan.A., Lijun Xu, Yuh-Jin Chao, and Kirkland Broach, 2000, "Numerical Simulation of Resistance Spot Welding Process", Journal of Numerical Heat Transfer, Part A, 37:425 –446.

[15]. Sun.X., and Dong.P., 2000, "Analysis of Aluminum Resistance Spot Welding Processes using Coupled Finite Element Procedures", AWS Welding Journal, August 2000: 215-221.

[16]. Tang.H., Hou.W., and Hu.S.J., 2002, "Forging Force in Resistance Spot Welding", Journal of Engineering Manufacture, Vol.216, pp. 315 –320.

[17]. Srikunwong.C., Dupuy.T.,and Bienvenu.Y., 2002, "Numerical Simulation of Resistance Spot Welding Process using FEA Technique", Journal of Science and Technology of Welding and Joining, Vol.49, pp.163-170.

[18]. Wenlong Mei, Vincent Li, and Lilong Cai, 2006, "Application of Finite Element Analysis in the Simulation of Spot Welding Process", ANSYS-China.

[19]. Quanfeng Song, Wenqi Zhang, And Niels Bay, 2005, "An Experimental Study Determines the Electrical Contact Resistance in Resistance Welding", AWS Welding Journal, pp.73-76.